Microstructure and mechanical characterisation of SLM processed Haynes® 230®

Microstructure and mechanical characterisation of SLM processed Haynes® 230®

T. Bauer[1], K. Dawson[2], A.B. Spierings[1], K. Wegener[3]

[1] Institute for rapid product development, Inspire AG, St.Gallen, Switzerland
[2] Centre for Materials and Structures, School of Engineering, University of Liverpool, Liverpool UK
[3] Institute of machine tools and manufacturing, Inspire AG, Tannenstrasse 3, 8092 Zurich, Switzerland

REVIEWED

Abstract

Selective Laser Melting (SLM) enables the production of complex near-net-shaped parts especially out of difficult to machine Nickel based alloys like Haynes® 230®. However, exact knowledge of the SLM processing windows and the corresponding mechanical properties is essential for a target-oriented part design as well as post process planning. Especially the high cooling rate of the small weld pool characterizes the SLM process and is known to cause material microstructures different to standard wrought or cast material.

Samples are built with different heat input levels and are analysed for their density, pore- and crack sizes. Optical and scanning electron microscope (SEM) and electron backscatter diffraction (EBSD) are used to characterize the material microstructure. Static tensile test samples were built in either 0° or 90° orientation for the evaluation of mechanical properties at room temperature and anisotropy as well as the influence of the different heat input levels are assessed.

It is shown that the alloy itself is well suited for the SLM process allowing the consolidation of nearly defect free material with improved mechanical properties with regards of yield and ultimate tensile strength compared to cast as well as wrought material.

Keywords: Selective Laser Melting, Additive manufacturing, Haynes® 230®, Nickel base alloys, Microstructure, Mechanical properties

Introduction

Selective Laser Melting (SLM) is a powder-bed based Additive Manufacturing technology which is becoming more and more popular especially for the production of complex shaped parts from high temperature alloys in turbine, aerospace as well as chemical industry. Haynes® 230® is used especially in the hot gas path of gas turbines (heat shields, combustion cans) as well as in high temperature applications in chemical or heating industry due to its high resistance against oxidation, nitridation and carburization [1, 2].

The SLM process is a generative production technology where the energy required to melt a powder shaped bulk material is supplied through a focussed laser beam. Typically a Nd:YAG

laser source with a wavelength of 1064 nm and power between 100 W and 400 W is used. The process is basically divided into the creation of a powder layer and its selective consolidation using the laser beam. Afterwards the substrate plate is lowered and the coating and consolidation process is repeated until the full part has been layer wise created.

High temperature alloys are prime examples for the advantages of additive manufacturing offering the possibility for the production of near-net-shaped complex parts thus drastically reducing the need for traditional machining as stated by Klocke et al. [3]. Gasser et al. [4] mention the increasing flexibility as well as creating new repair and servicing strategies. Inconel® 718 is the most common high temperature alloy used for SLM processing [5-10]. Therefore a high number of publications dealing with microstructure and mechanical properties are available. Amato et al. [8] have shown that the yield and ultimate tensile strength of SLM produced Inconel® 718 can outperform the values for conventional material while being deficient in regards of elongation at break. A further high temperature alloy well known in the SLM-community is Inconel® 625 which has been intensively characterised by Murr et al. [11] as well as Helvajian et al. [12] discussing microstructure and static and dynamic properties. For both of the aforementioned alloys ASTM released standards for the additive manufactured materials [13, 14]

Due to the very low content of Titanium and Aluminium (see Table 1) which are identified as γ′-formers as mentioned by Davis et al. [15], Haynes® 230® is known for offering good welding characteristics that exceed the one of Inconel® 625 and Inconel® 718. Nonetheless there is hardly any literature available on the behaviour of SLM processed Haynes® 230®.

The aim of the following study is the determination of the basic processing window, the mechanical properties as well as the corresponding microstructure. Furthermore different processing windows are proposed in order to accommodate different requirements or post processing procedures such as hot isostatic pressing (HIP).

Material and Methods

The Haynes® 230® alloy used for this study was sourced through LPW Technology Ltd. showing the chemical composition displayed in Table 1. The powder was gas-atomized using argon gas resulting in mostly spherical particles. The particle size distribution is between 15 µm and 45 µm.

Table 1: Chemical composition of Haynes® 230®

Element	Ni	Cr	W	Mo	Fe	C	Mn	Si	Al	Other
wt. %	Bal.	22.81	14.38	2.1	1.86	0.11	0.75	0.54	0.37	0.235

All samples were produced on a Concept Laser machine type M2 equipped with a 200 W Nd:YAG fibre laser operating in cw-mode with a Gaussian beam shape. A full factorial experimental design was chosen (see Table 2) using a wide range of hatch distances (75 µm to 105 µm) as well as scan speeds (450 mm/s to 1200 mm/s) and a fixed layer thickness of 30 µm.

The laser power was kept at the machine maximum output of 200 W in order to meet productivity requirements.

Table 2: Parameter range used for SLM of Haynes® 230

	Layer thickness t (µm)	Scan speed v_s ($^{mm}/_s$)	Hatch distance d (µm)	Volume energy density (J/mm^3)
Haynes® 230	30	450 - 1200	75 – 105	53 - 186

For the investigation of density as well as microstructure test cubes with the dimension of 10x10x10 mm^3 are built with a meander like scanning strategy (see Figure 1). The scan direction is alternated by 90° from layer to layer in order to increase relative density as stated by Kruth et al. [16]. The samples were placed randomly on the metal base plate. The volume energy density E_{vol} (1) is calculated from the main influencing processing parameters of the process – the laser power P (W), scan speed v_s (mm/s), layer thickness t (mm) as well as the hatch distance d (mm) :

$$E_{vol} = \frac{P}{v_s \cdot t \cdot d} \qquad (1)$$

The measurement of material density was carried out using the Archimedes method with acetone as measurement fluid according to the recommendations of Spierings et al.[17] and the reference value for the density was set to 8.97 g/cm^3 according to the bulk material specification by Haynes Int.[1].

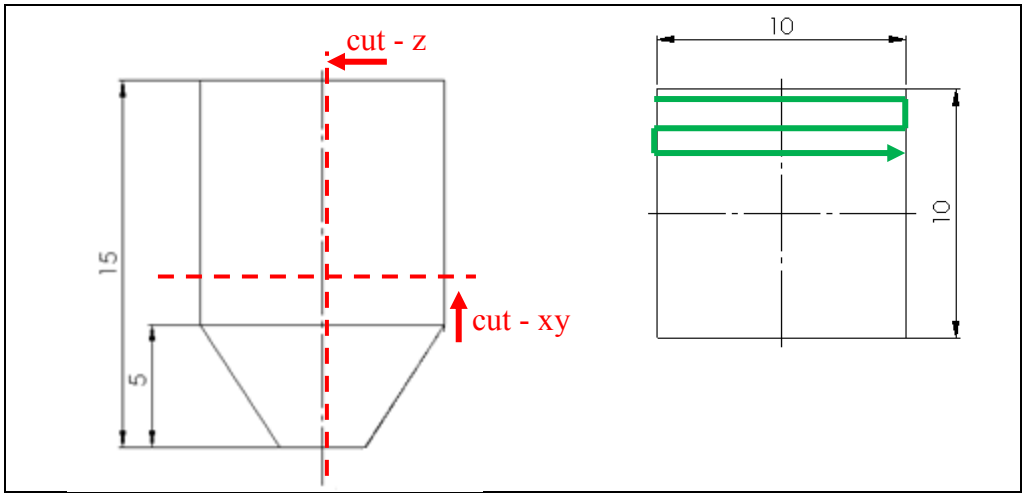

Figure 1: Applied cutting directions (left) scanning strategy (right)

The specimens were cross sectioned to expose planar surfaces parallel to the build direction (see Figure 1) as well perpendicular to expose the xy-plane. Samples were prepared using standard metallographic techniques and a final polish was applied using colloidal silica.

Optical microscopy was carried out on a Keyence VHX-1000 with 200-times magnification. Scanning electron microscopy (SEM) and electron backscattered diffraction (EBSD) analysis were performed in an FEI Helios 600i microscope fitted with an EDAX DigiView EBSD system.

The mechanical testing at room temperature was performed on a Walter&Bai tensile testing machine type LFV-25 equipped with a clip gauge. Sample geometry and number was chosen in agreement with the recommendation VDI-3405 [18]. The test samples with a gauge diameter of 5 mm have been built in 0°-orientation (vertical), 90°- orientation (horizontal) and were machined in accordance with the specification of DIN 50125 A-5x25 [19].

Results

SLM processing and relative density

The powder used showed a good flowability with a Hausner ratio 1.15 and an avalanche angle of 45° determined using the revolution powder analyser method investigated by Amado et al. [20]. Thus the recoating process was consistent creating a smooth surface for processing (see Figure 2).

Samples with a high energy input (more than 115 J/mm^3) showed extensive weld spattering as well as increased creation of welding fumes during the process which can be critical for longer build times with regards to filter condition and contamination of the laser window leading to an unstable build process.

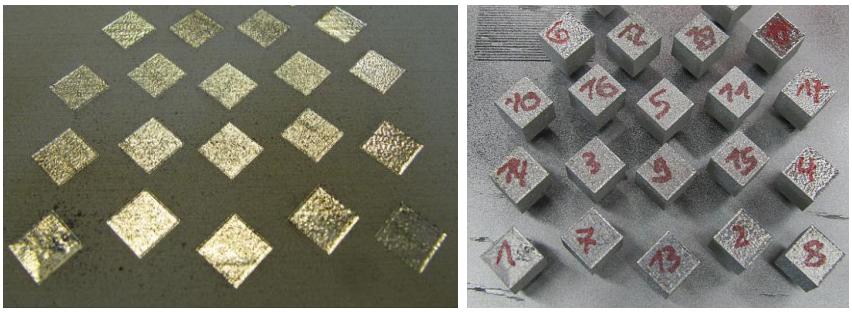

Figure 2: SLM powder bed (left) and finished test samples (right)

A relative density > 99 % could be reached using energy densities higher than 66 J/mm^3 (see Figure 3). Below this energy level the relative density drastically dropped leading to an increased size and amount of internal pores (see Figure 4). At energy densities over 115 J/mm^3 the relative density reached values over 99.8 % which is consistent with the evaluated micrographs. Further energy input did not lead to a major increase in relative density.

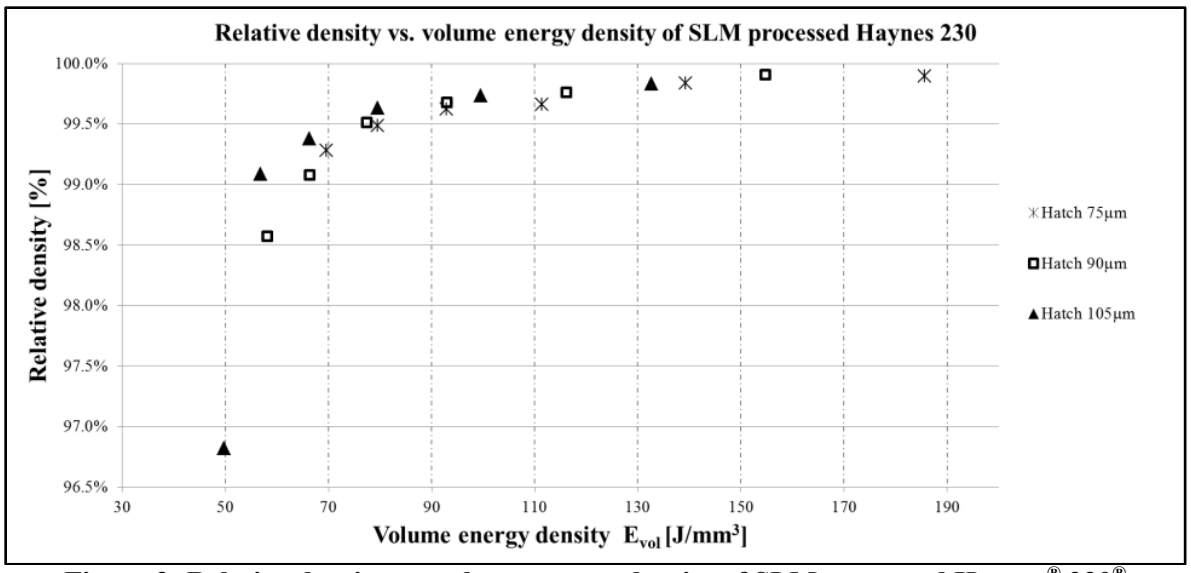

Figure 3: Relative density vs. volume energy density of SLM processed Haynes® 230®

Figure 4 shows an increase of porosity as well as an increase of pore size with decreasing energy input. Haynes® 230® shows a particularly steep decrease in relative density below 66 J/mm^3 energy density. Nearly no cracking could be observed for the optical evaluated micrographs which will create a nearly full dense material after HIP-processing.

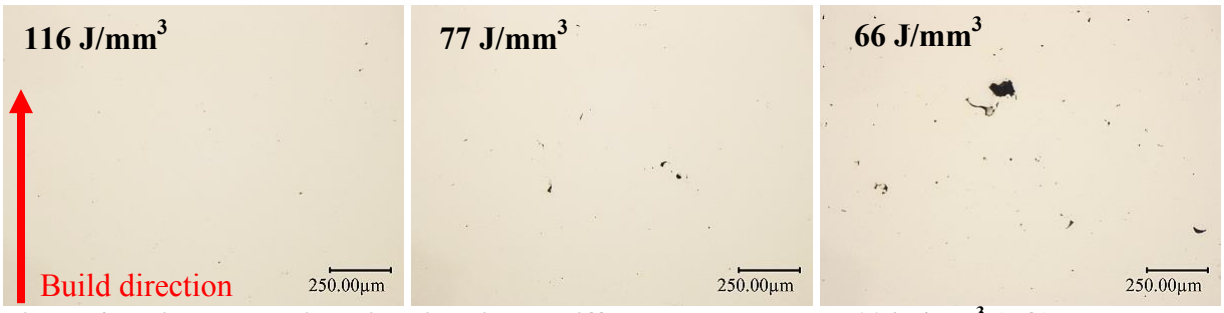

Figure 4: Micrographs in build direction at different energy levels; 116 J/mm^3 (left); 77 J/mm^3 (middle); 66 J/mm^3 (right)

Based on the results of density tests and optical microscopy 3 parameter windows were selected in order to provide a solution for different requirements. The low energy input parameter targeted production of builds with a relative density of 99%, whilst retaining high productivity and a defect size which would permit full curing by HIP treatment. The medium energy input level of 77.3 J/mm^3 focussed on providing a relative density of approximately 99.4 % whislt offering a good compromise between process reliability, productivity and mechanical properties. The high energy level of 116 J/mm^3 targeted optimisation of build density in order to create a nearly defect free part in the as built condition; employing similar build strategies might mitigate the requirement of post processing by HIP.

Tensile testing

Three sets of samples, each built using a different laser energy input, were produced. Each sample set comprised of 10 specimens, of which 5 were built vertically and 5 in a horizontal configuration. The samples were validated by their density. The results are presented in Table 3 and Figure 5.

Table 3: Results of static tensile tests for SLM processed Haynes® 230®

	High energy input		**Medium energy input**		**Low energy input**	
Rel. density [%]	99.60±0.23		99.38±0.20		98.87±0.30	
Volume Energy density [J/mm^3]	116		77		66	
	Vertical	Horizontal	Vertical	Horizontal	Vertical	Horizontal
Yield strength (0.2%) [MPa]	656±4	798±5	681±2	794±6	702±6	798±10
Tensile strength [MPa]	941±2	1102±6	979±5	1087±5	991±19	1077±11
Young's Modulus [GPa]	152±1	205±4	165±3	201±2	179±4	201±3
Elongation at Break [%]	32±3	28±1	25±4	25±2	16±4	21±2

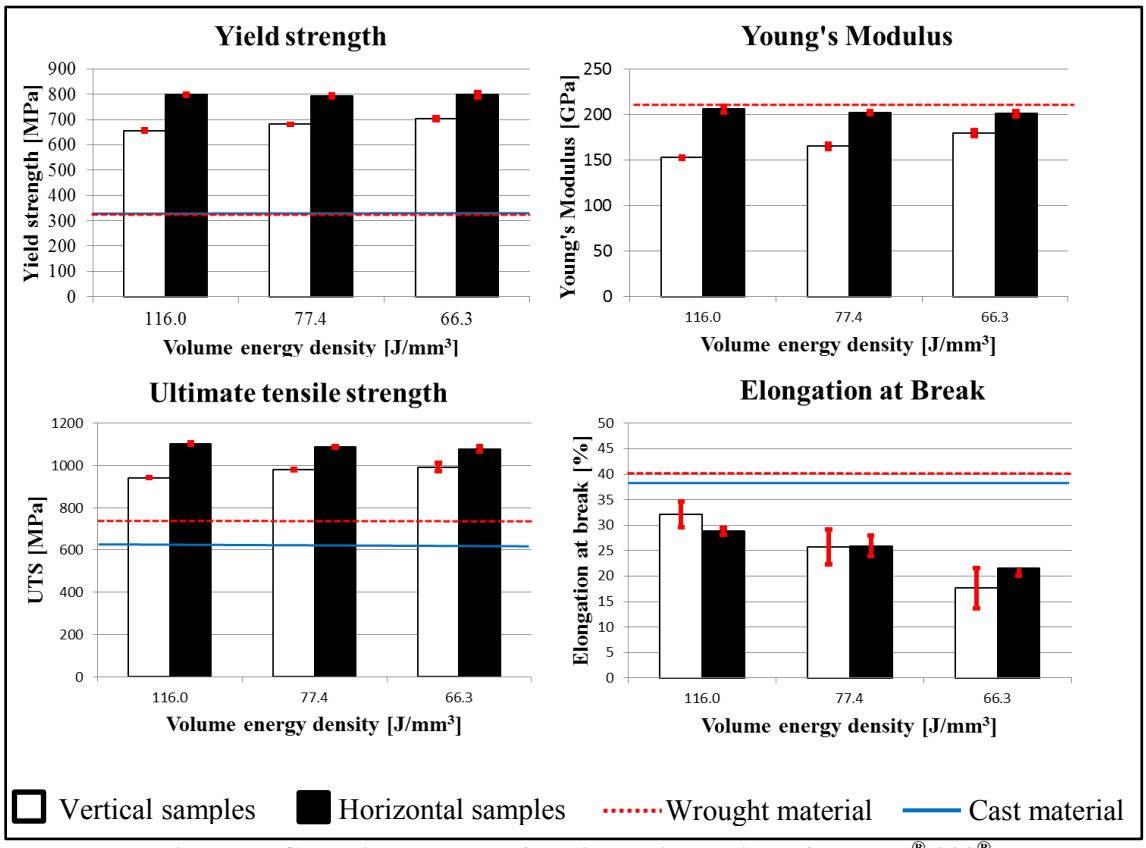

Figure 5: Graphical results of static tensile testing of Haynes® 230®

There was only a minor influence of the energy density on ultimate tensile strength, yield strength or the Young's modulus of the horizontal built samples. The median yield strength, ultimate tensile strength and Young's Modulus were measured at 796 MPa, 1089 MPa and 202 MPa respectively for the three build energies. As a result of the increasing porosity and interlayer bonding errors the elongation at break decreases with lower energy input from 32 % at 116 J/mm^3 to 21 % at 66 J/mm^3. Nonetheless the values of yield strength and ultimate tensile strengths are significantly higher than the required values for cast according to Haynes International [1] and wrought material (ASTM B435 [21]). Elongation to break figures for the horizontal builds, irrespective of build energy, were inferior to those published for cast alloy.

The vertical built samples displayed inferior mechanical properties to those shown by the horizontal builds whilst exhibiting a typical anisotropy for the SLM process of 14 % (median difference of all values) – depending on the energy input as well as the different mechanical properties. Nearly isotropic properties could be reached on the medium energy input level for the elongation at break while still keeping the anisotropy at yield strength, ultimate tensile strength as well as Young's modulus.

Microstructural characterisation

Specimens of SLM processed Haynes® 230® in the as-built condition were analysed. Optical microscopy indicated the greatest density was achieved using the highest energy density and porosity increased with decreasing energy input. Cracks and voids observed at 66 J/mm^3, the fastest build rate analysed, appeared to be related to the incomplete melting of powder particles.

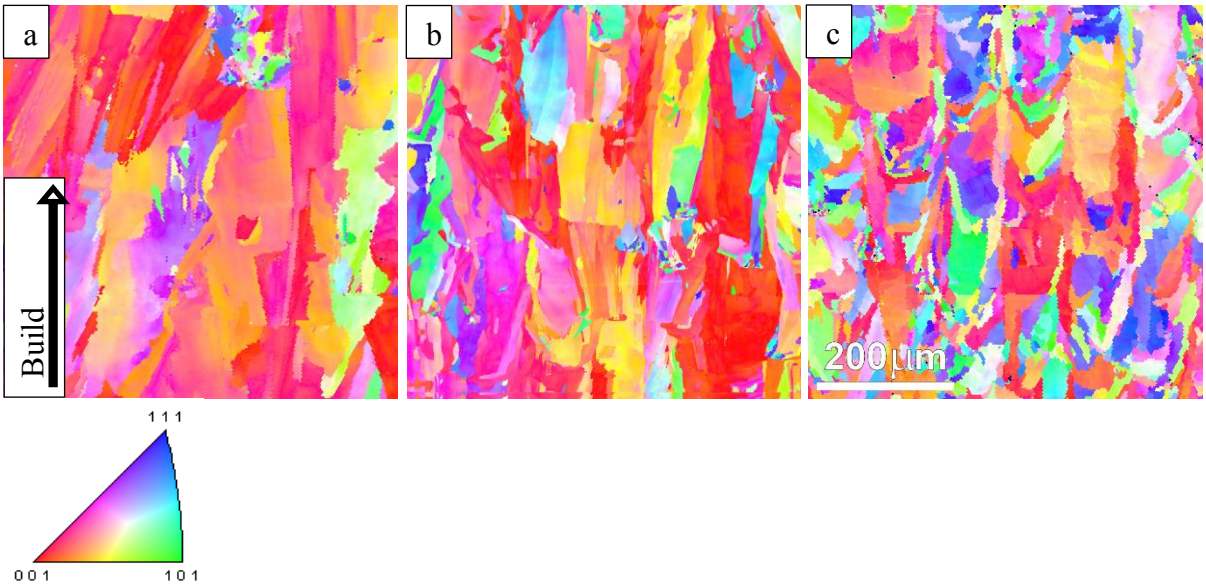

Figure 6: Inverse pole figure EBSD maps of Haynes® 230® alloy SLM builds made using (a) 116 J/mm^3, (b) 77 J/mm^3 and (c) 66 J/mm^3

EBSD was used to determine grain size distributions and the crystallographic texture of SLM builds. All builds displayed columnar grain structures with the long axes of grains approximately parallel to the build direction (Figure 6 a, b and c). Columnar grains, separated by high angle boundaries, exhibited lengths which spanned multiple layers depending on the energy input

during the build. The mean grain size decreased with lower energy input; this appeared to be due to a break-up of the epitaxial columnar growth. All builds displayed a solidification fibre texture with a preferred orientation of growth described by <100>γ parallel to the build direction. However, the texture was less distinct in the fast scan builds resulting in a more chaotic microstructure. Close examination revealed that cracks and powder particles which had not melted completely often resulted in the nucleation and growth of randomly oriented crystals. However, the competitive nature of growth resulted in favourably oriented grains dominating the new growth, hence new columnar grains were developed.

SEM images which were formed using backscattered electrons displayed both channelling contrast and z-contrast which revealed dendritic and cellular subgrain structures within the columnar grains. Also apparent was the redistribution of solute elements to interdendritic and cellular boundary regions. It was not possible to determine the composition of the segregated material by EDS analysis, as the width of enriched bands was in the order of only 100nm; however, z-contrast imaging indicated that the average atomic weight of the alloy in the segregated regions was greater than that of the alloy matrix (Figure 7b). It is likely that these regions were enriched in tungsten and chromium; Ernst [22] reports similar enrichment of subgrain boundaries in the solidification structures of Haynes® 230® GTAW welds. Due to the fast cooling rates experienced in all of the SLM built structures analysed, dendrite spacings were restricted to only 1µm to 2µm which is displayed in Figure 7.

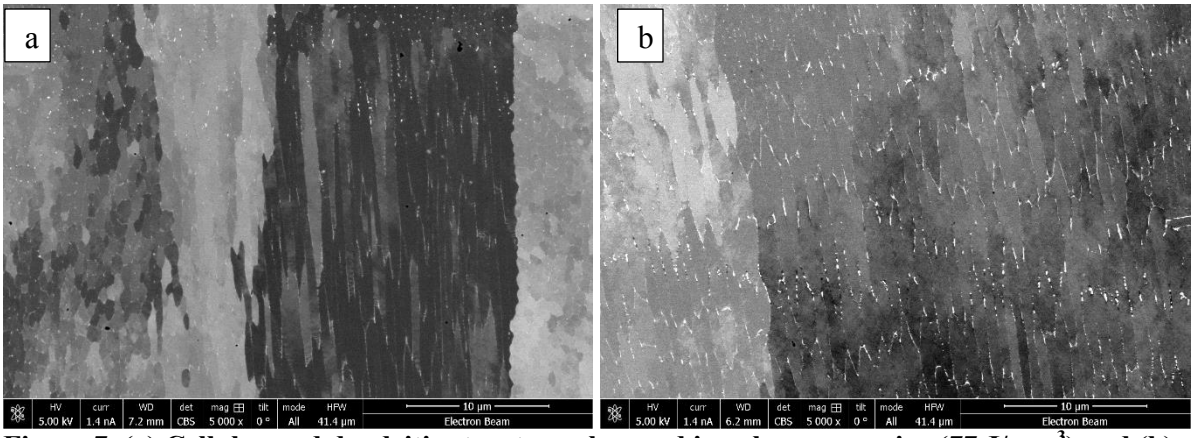

Figure 7. (a) Cellular and dendritic structure observed in columnar grains (77 J/mm^3) and (b) segregation forming high-z regions at subgrain boundaries.

Conclusion

It has been demonstrated that in combination with Selective Laser Melting Haynes® 230® can be processed using a wide range of parameters to obtain nearly full density material. The resulting material offers significantly improved mechanical properties regarding yield and tensile strength over casted and wrought material. Nonetheless it shows a process typical embrittlement and does not fulfil the requirements for the elongation at break in the as built condition. The as-built microstructures were comprised of columnar grains elongated in the build direction and segregation to grain and sub-grain boundaries was evidenced. As a result of the anisotropic microstructures, build configuration dependent differences were measured in mechanical

properties; the as built material displayed a median 14% variance between the horizontal and vertical build directions. In conclusion the material is well suited for the SLM process also creating the possibility for new repair and supply chain strategies in the future.

Outlook

Future work will explore the effects of different heat treatment regimes, their corresponding microstructural changes and an in-detail analysis of the segregation that occurs at the SLM processed material.

Acknowledgements

The work was funded by European Commission within the FP7-Project OXIGEN,
Grant No. NMP3-SL-2011-310279.

Literature

1. Haynes International, *Haynes 230 Alloy*. 2007: Kokomo, Indiana (USA).
2. Haynes International, *Fabrication of Haynes and Hastelloy solid-solution-strenghtened high-temperature alloys*. 2002: Kokomo, Indiana (USA).
3. Klocke, F., Klink, A., Veselovac, D., Aspinwall, D.K., Soo, S.L., Schmidt, M., Schilp, J., Levy, G., and Kruth, J.-P., *Turbomachinery component manufacture by application of electrochemical, electro-physical and photonic processes.* CIRP Annals - Manufacturing Technology, 2014. **63**(2): p. 703-726.
4. Gasser, A., Backes, G., Kelbassa, I., Weisheit, A., and Wissenbach, K., *Laser Additive Manufacturing.* Laser Technik Journal, 2010. **7**(2): p. 58-63.
5. Sufiiarov, V.S., Borisov, E.V., and Polozov, I.A., *Selective Laser Melting of the Inconel 718 Nickel Superalloy.* Applied Mechanics and Materials, 2014. **698**: p. 333-338.
6. H.Helmer, Hartmann, N., Körner, C., and Singer, R.F. *Relation Between Processing Strategy, Grain Structure and Mechanical Properties in Superalloy Inconel 718 Processed by Selective Electron Beam Melting*. in *DDMC*. 2014. Berlin: Fraunhofer
7. Wang, Z., Guan, K., Gao, M., Li, X., Chen, X., and Zeng, X., *The microstructure and mechanical properties of deposited-IN718 by selective laser melting.* Journal of Alloys and Compounds, 2012. **513**: p. 518-523.
8. Amato, K.N., Gaytan, S.M., Murr, L.E., Martinez, E., Shindo, P.W., Hernandez, J., Collins, S., and Medina, F., *Microstructures and mechanical behavior of Inconel 718 fabricated by selective laser melting.* Acta Materialia, 2012. **60**(5): p. 2229-2239.
9. Amsterdam, E. and Kool, G.A. *High Cycle Fatigue of Laser Beam deposited Ti64 and IN718.pdf*. in *25th ICAF Symposium*. 2009. Rotterdam.
10. Rao, G.A., Kumar, M., Srinivas, M., and Sarma, D.S., *Effect of standard heat treatment on the microstructure and mechanical properties of hot isostatically pressed superalloy inconel 718.* Materials Science and Engineering: A, 2003. **355**(1-2): p. 114-125.

11. Murr, L.E., Martinez, E., Gaytan, S.M., Ramirez, D.A., Machado, B.I., Shindo, P.W., Martinez, J.L., Medina, F., Wooten, J., Ciscel, D., Ackelid, U., and Wicker, R.B., *Microstructural Architecture, Microstructures, and Mechanical Properties for a Nickel-Base Superalloy Fabricated by Electron Beam Melting Inconel 625.* Metallurgical and Materials Transactions A 2011. **42**(11): p. 3491-3508.
12. Helvajian, H., Piqué, A., Wegener, M., Gu, B., Witkin, D.B., Adams, P., and Albright, T., *Microstructural evolution and mechanical behavior of nickel-based superalloy 625 made by selective laser melting.* 2015. **9353**: p. 93530B.
13. ASTM. F 3056: Standard specification for Additive Manufacturing Nickel Alloy (UNS N06625) with powder bed fusion. 2014.
14. ASTM. F 3055: Standard specification for Additive Manufacturing Nickel Alloy (UNS N07718) with powder bed fusion. 2014.
15. Davis, J.R., *ASM Specialty Handbook - Nickel, Cobalt, and Their Alloys*. 2000, ASM International.
16. Kruth, J.P., Badrossamay, M., Yasa, E., Deckers, J., Thijs, L., and Van Humbeeck, J. *Part and material properties in selective laser melting of metals*. in *16th International Symposium on Electromachining*. 2010. Shanghai, China.
17. Spierings, A.B., Schneider, M., and Eggenberger, R., *Comparison of density measurement techniques for additive manufactured metallic parts.* Rapid Prototyping Journal, 2011. **17**(5): p. 380-386.
18. VDI. 3405: Additive Fertigungsverfahren: Grundlagen, Begriffe, Verfahrensbeschreibungen. 2014.
19. DIN. 50125: Prüfung metallischer Werkstoffe - Zugproben. 2009.
20. Amado, A., Schmid, M., Levy, G., and Wegener, K., *Advances in SLS powder characterization*, in *Solid Freeform Symposium*. 2011: Austin (TX).
21. ASTM. B 435: Standard Specification for UNS N06002, UNS N06230, UNS N12160, and UNS R30556 Plate, Sheet, and Strip. 2011.
22. Ernst, S.C. *Weldability Studies of Haynes 230 Alloy*. in *72nd Annual AWS Meeting*. 1994. Detroit.